



# Experimental study of the effect of the length-to-width ratio and skewness angles of the pier installed at the bend on scour pattern

Danesh Dehghan<sup>1</sup> · Mohammad Vaghefi<sup>2</sup> · Masoud Ghodsian<sup>3</sup>

Received: 17 July 2020 / Accepted: 8 February 2021 / Published online: 20 February 2021  
© The Brazilian Society of Mechanical Sciences and Engineering 2021

## Abstract

One of the causes of the destruction or damage of many bridges in the world is the local scour around the bridge piers. Accordingly, research on effective factors on the scouring pattern around the bridge piers is a necessity. In this study, the parameters of the scour hole created around rectangular piers, such as the depth, area and volume of the scour hole, and the effects of increasing the rectangular pier's length-to-width ratio and its skewness angle towards the banks on scour hole parameters, bed topography changes and the downstream straight path in a 180° sharp bend has been investigated. The results showed that in a 180° sharp bend, the length of the rectangular pier should be at least 3 and at most 5 times its width. The pier with a length-to-width ratio of 3 had a better performance in terms of reducing scouring along the bend. The maximum depth of the scour hole around the piers occurs when the piers are located at 90°. Increasing the angle of attack caused by skewing the pier towards the inner and outer bank at 90° increases the depth and volume of the scour hole.

**Keyword** Rectangular pier · Length-to-width ratio of pier · Skewed pier · Local scour · 180° bend

## 1 Introduction

Scour is one of the most important issues in river engineering. When a bridge is set up over a river, it necessitates implementation of bridge piers inside the river bed; hence, the piers are exposed to flow attack and the resulting scour. The bridge pier also causes variations to the flow pattern, and these variations lead to an increase in the sediment transport capacity in the water environment and will eventually result in the scour phenomenon. Determining the scour

depth plays a decisive role first in indicating the destructive potential of the flow around the pier, and second in designing the piers dimensions. Therefore, predicting the scour pattern and determining the maximum scour depth and generally the downstream topography play a decisive role in the future behaviour of the river. The scour around the bridge pier has a highly complicated mechanism and it has been addressed by different researchers. The following are instances of experimental studies conducted on the issue of scouring around bridge piers placed in straight channels.

Chiew and Melville [1] studied local scour around cylindrical piers. The results indicated that the equilibrium scour depth increases in a linear fashion up to a value of 50 by increasing the dimensionless ratio of the pier diameter to the average particle size, and thereafter the equilibrium scour depth value is independent from this ratio. Dargahi [2] examined the scour mechanism around a cylindrical pier and concluded that the scour process around the pier occurs in three phases: the scour onset, the initial scour and the gradual reduction. The scour onset occurs when a steady bed is changed into a mobile bed and a scour hole is created around the pier in the second phase due to presence of a horseshoe vortex. Kumar et al. [3] utilized collars and slots to reduce scour around a circular bridge pier. They concluded that the amount of scour reduction due to the

---

Technical Editor: Erick Franklin.

✉ Mohammad Vaghefi  
Vaghefi@pgu.ac.ir

Danesh Dehghan  
daneshdehghan73@gmail.com

Masoud Ghodsian  
ghods@modares.ac.ir

<sup>1</sup> Department of Civil Engineering, Persian Gulf University, Shahid Mahini St, 7516913798 Bushehr, Iran

<sup>2</sup> Department of Civil Engineering, Faculty of Engineering, Persian Gulf University, 7516913798 Bushehr, Iran

<sup>3</sup> Faculty of Civil and Environmental Engineering, Tarbiat Modares University, Tehran, Iran

slot is greater than the collar so that the most effective function of the slot is achieved when it is positioned at the  $20^\circ$  angle of attack and near the bed surface. Bozkus and Yildiz [4] placed an inclined cylindrical pier longitudinal to the flow in downstream direction and showed that increasing the pier inclination angle in downstream direction decreases the scour. Sheppard et al. [5] investigated the maximum scour depth around a cylindrical pier with three different diameters and concluded that the maximum scour depth at the end of the experiment occurs usually at a location other than that during the experiment. Zarrati et al. [6] studied the effect of the collar width on scour reduction around a skewed rectangular pier. The results indicated that wider collars resulted in further reduction in the scour depth around the pier. In addition, skewing the pier reduced the efficiency of the collar around the pier. Zarrati et al. [7] implemented a collar around circular and rectangular piers and proposed that the collar functioned better in reducing scour around a single rectangular pier than a continuous collar around two circular piers. Furthermore, combination of the collar and riprap significantly reduced scour around the piers. Bozkus and Cecme [8] investigated the scour depth of twin inclined and vertical piers longitudinal to the flow for different flow depths. The results showed that the scour depth around inclined piers decreased in comparison with that around the vertical piers. Also, the scour depth for grouped piers significantly decreased compared to that for a single pier. Mashahir et al. [9] examined the effect of increasing the rectangular pier length on the efficiency of the collar with constant dimensions in reducing the scour around the pier. The results indicated that increasing the pier length lessens the effectiveness of the collar for scour reduction. Further, increasing the skewness angle of the pier increases the scour depth around the pier and reduces the collar efficiency. Chaudhuri and Debnath [10] investigated the scour process around cylindrical and square piers and concluded that the scour mechanism at the cylindrical pier shows that the scour initiates from the pier sides; however, in the square pier, it initiates from the corners of the upstream-facing wall and extends to the pier downstream end. Ismail et al. [11] studied the scour around a single pier and two piers with side-by-side arrangement and showed that increasing the piers diameter increases the scour depth, and by reducing the distance between the two piers, the scour depth around the piers increases. Aghaee-Shalmani and Hakimzadeh [12] addressed the scour depth at conical piers with circular and elliptical sections and different lateral slopes. They showed that the upstream and downstream scour depths for conical piers with a lateral slope angle of  $15^\circ$  to the vertical axis, respectively, decrease by about 36 and 53% compared to those for a circular pier. Ahmad et al. [13] examined the skewness angle of a rectangular pier towards the channel walls. The results showed that increasing the skewness angle

towards the wall increased the maximum scour depth that had happened near the pier nose. Fael et al. [14] studied the effect of the pier shape and the pier alignment on the scour depth around it. They concluded that the shape coefficient should be considered 1 for rectangular piers with round noses and 1.2 for rectangular piers with sharp corners. Shukur and Obeid [15] examined the role of the pier shape in minimizing the scour hole around the pier. The results indicated that the scour depth upstream of the pier was directly related to the shape of the pier nose, and the maximum and minimum scour depths had, respectively, occurred around rectangular and streamline piers. Talib et al. [16] investigated the effect of piers shape and the Froude number on the amount of scour around the pier. The results showed that the maximum scour occurred in front of the pier nose, and increasing the flow velocity increased the maximum scour. Furthermore, a formula has been obtained by using dimensional analysis and the available data which highly correspond with the experimental results. Shukri [17] examined the local scour depth around a circular pier with different diameters and concluded that the scour depth increased by increasing the pier diameter for sediments with the same particle diameter. In addition, reducing the average size of the sediments increased the maximum scour depth. Abozeid et al. [18] compared the effect of a slot made on a rectangular pier with a group of circular piers on scour reduction around the piers. They found that the dimensions of the scour hole created around the grouped piers are smaller than those at the rectangular pier with a slot so that the grouped piers caused a 93% reduction in the scour hole depth. Ahmed and Khassaf [19] studied the effect of the pier shape and the level of the pier foundation relative to the initial bed on the scour around different shapes of piers. The results indicated that the scour depth depended on the foundation level, and the shape of the pier and the foundation. The minimum scour depth occurred around a hexagonal pier and foundation. Also, installation of the foundation beneath the initial bed caused a further reduction in the scour around the pier.

Among the important factors causing scour around the bridge piers are downflows, a horseshoe vortex in the front and wake vortices behind the pier. Once the flow collides with the pier, due to the pressure gradient in the vertical direction, the flow is diverted downwards. After it collides with the bed, it causes a scour hole around the pier by creating a horseshoe vortex in front of it. This hole is extended towards the downstream side of pier by the wake vortices. Digging the scour hole continues until the vortices energy is depleted as the volume of water inside the scour hole increases. Then the scour depth reaches equilibrium [6]. The main characteristic of the flow in the bend is the presence of a spiral flow, which forms a combination of secondary flow and a longitudinal velocity profile. The collision of these flows with the pier makes the flow pattern more complex,

and, as a result, the scour pattern here differs from that of the straight path. Factors such as pier shape and geometry, pier position and the skewness angle of the pier to the flow influence the scour around the pier in the bend. A more accurate study on the parameters affecting the bed topographic changes, such as the maximum scour depth around the piers and changes on the inner and outer banks, are factors that need to be addressed in the bend-shaped path. Instances of the studies conducted on the flow and scour pattern and sediment transport around piers located at bends:

Odgaard and Bergs [20] examined the dynamic properties of the flow in a  $180^\circ$  bend and concluded that owing to a change in the channel curvature at the bend entrance, the flow acceleration has a significant effect on the flow in the bend. Sui et al. [21] investigated the role of hydraulic factors in scour development at the walls of a  $90^\circ$  bend. As suggested by the results, generation of the secondary and spiral flows at the upstream centre of the bend and towards the inner wall causes scour at the outer wall and sedimentation at the inner wall of the bend. Masjedi et al. [22] carried out an investigation of the maximum scour depth around a rectangular pier at different positions of a  $180^\circ$  bend and found that the maximum scour depth at the  $60^\circ$  angle of the bend occurred around the rectangular pier. Also, increasing the Froude number increased the scour depth in all positions. Ben Mohammad Khajeh et al. [23] studied the depth and location of the scour around inclined and vertical cylindrical piers in a  $180^\circ$  bend. They concluded that the maximum and the minimum scour depths, respectively, occurred around the pier inclined towards the outer bank and the inner bank, and installation of the pier inclined towards the outer bank led to formation of alternating sedimentary dunes at the downstream side of the pier in the vicinity of the inner bank. Helmy et al. [24] examined the effect of pier shape and rotation angle of pier relative to the flow direction on the maximum scour depth around a pier located in a  $30^\circ$  bend. They concluded that all piers have the best performance against reducing scour depth by being longitudinal to the flow direction, while the hexagonal pier requires a rotation angle of  $2.5^\circ$  relative to the flow direction for better performance. Maatooq and Mahmoud [25] conducted a study of the maximum scour depth around a rectangular pier at different positions of a  $180^\circ$  bend. They found that the maximum scour depth occurred with the pier installed at the  $90^\circ$  position of the bend, and by skewing the pier towards the inner bank, compared to the outer bank, the values of scour depth increased. Vaghefi et al. [26] investigated the role of base-level fall at the bend entrance in scour reduction around a rectangular pier in a  $180^\circ$  sharp bend and indicated that creating a fall at the upstream side of the pier increased the flow depth and decreased the velocity in the vicinity of the pier; hence, the maximum scour hole depth and volume, respectively, decreased by 73 and 97%. Vaghefi et al.

[27] studied the scour around cylindrical piers transverse and longitudinal to the flow direction at different positions of a  $180^\circ$  sharp bend. The results indicated that placing the piers at the  $60^\circ$  position, in both cases, led to the maximum scour hole area around the piers, and sedimentary dunes developed downstream of the piers. Eghbali et al. [28] examined the temporal variations of the scour depth and bed topography around a group of piers transverse to the flow direction at the  $60^\circ$  position of a  $180^\circ$  bend and showed that in time, the location of the maximum scour depth tends from the inner bank to the outer bank. Asadollahi et al. [29] conducted a study of scour and flow patterns around a group of piers located at different positions of a  $180^\circ$  sharp bend both experimentally and numerically and concluded that the position of the piers in the bend does not influence the location and the amount of the maximum scour depth. In addition, the maximum secondary flow power around the piers in the first half of the bend is greater than that in the second half. Mahmoud [30] studied the role of pier shape, rotation angle of pier relative to the flow direction, the Froude number and particles with different diameters in minimizing the scour depth around a pier in a  $30^\circ$  bend. The results showed that a hexagonal pier with a rotation angle of  $2.5^\circ$  resulted in 22–35% reduction in the maximum scour depth under different conditions in comparison with a rotation angle of  $0^\circ$ . Moghanloo et al. [31] examined the effect of collar thickness on the flow pattern around an oblong pier located at the  $90^\circ$  position of a  $180^\circ$  sharp bend. As suggested by the results, increasing the thickness of collar placed at a level equal to 0.4 times the pier width and that located at a level higher than the initial bed level severely decreased the kinetic energy at the upstream side of the pier and increased the streamlines orientation towards the bed. Hence, the scour hole depth increased. Moghanloo et al. [32] examined the role of thickness and level of the collar at the oblong pier in reducing the dimensions of the scour hole developed around the pier in a  $180^\circ$  bend and concluded that increasing the collar thickness at the levels above the bed increased the scour depth. Also, placing the collar near and below the initial bed level further reduced the scour hole dimensions around the pier compared to the pier without a collar. Rasaei et al. [33] studied the depth and volume of the scour hole around circular and cubic piers in a  $90^\circ$  convergent bend with a central radius of 1.7 m. The results indicated that the maximum depth and volume of scour hole around the piers occurred when the piers were installed at the  $75^\circ$  angle of the bend. Sedighi et al. [34] examined the scour around convergent and divergent circular piers at different positions of a  $180^\circ$  sharp bend governed by different flow regimens and concluded that moving the convergent circular piers from the first half of the bend to the second half increased the maximum scour depth.

The above-mentioned studies indicated that various factors are involved in the scour process around bridge piers installed at bend paths. One of the effective parameters less often studied is the ratio of pier length to pier width. This ratio plays a substantial role in creating and empowering the system of vortices around the pier and hence the amount of scour and bed topography changes. This study is innovative in addressing the effect of the ratio of length to width of rectangular piers with round noses, with bridge piers installed at different positions of a 180° sharp bend. In this study, topics such as the downstream straight path topography changes, the depth and location of the maximum scour and sedimentation, the values of area and volume of the scour hole around the piers, and the effect of a skewed pier with different angles relative to the flow direction on scour were studied and analysed.

## 2 Material and methods

Experiments were carried out at the hydraulic laboratory of Persian Gulf University in Bushehr. The main channel had a straight upstream path with a length of 6.5 m and a straight downstream one which was 5 m long. A 180° channel was placed between the two paths. The cross section of the rectangular channel had a width of 1 m and a height of 0.7 m and the bend central radius to width ratio was 2 [35]. A schematic view of the experimental flume is shown in Fig. 1a.  $R$  represents the inner radius of bend. The bed and sides of the channel were made of glass, supported by a metal frame. The flow measurements were made with an ultrasonic flow meter. A gate was placed at the end of the main channel to control the flow depth. The bed sediments with an average size of  $d_{50} = 1.5$  mm, a thickness of 0.3 m and the standard deviation of  $\sigma = \sqrt{d_{84}/d_{16}} = 1.14$  were used and covered the entire channel.

The rectangular piers had round nose and tail, and they were made of PVC. The piers width was  $b = 0.05$  m and their length was  $L = 0.05, 0.1, 0.15, 0.2, 0.25$  and  $0.3$  m. Therefore, the  $L/b$  ratios of those piers, respectively, were 1, 2, 3, 4, 5 and 6. The parameter of  $\theta_p = 60, 90$  and  $120^\circ$  was chosen to indicate the location of the piers and its effect on scouring in the bend with the pier. In addition, the parameters of  $\alpha = \pm 15, \pm 30, \pm 45, \pm 60, \pm 75, 90^\circ$ , respectively, showed the skewness of the pier towards the inner and outer banks (Fig. 1b).

At the onset of the experiment, temporal variations of the scour hole depth in front of the pier nose were collected by the temporal variations harvesting device made of a metal body, a ruler and a moving indicator. In addition, the depth and location of the maximum scour and sedimentation, and bed topography changes were collected by bed topography harvesting laser device with a  $\pm 1$  mm precision rate at the

end of the experiment. Smaller meshes were used around the piers to harvest the bed topography. Figure 1c, d illustrates the maximum scour temporal variations harvesting device and the bed topography harvesting laser device, respectively.

All experiments were carried out in close proximity to the bed material movement threshold. According to Chiew [36], if  $y/b$  is greater than 3 (where  $y$  is the flow depth and  $b$  denotes the pier width), the water depth will not affect the scour hole depth. The experiments were carried out at a discharge of  $0.07 \text{ m}^3/\text{s}$ , the flow depth at the beginning of the bend was about 0.18 m, and  $u/u_c$  was 0.98 ( $u$  and  $u_c$  are average flow velocity and flow velocity at the threshold motion of particles, respectively). In order to determine the relative equilibrium time for conducting the experiments, a 34-h equilibrium time experiment with a rectangular pier located at the  $90^\circ$  position was performed. Almost 95% of the maximum scouring occurred in the first 15 h of the experiment, which is consistent with the results of Melville and Chiew [37]. Therefore, 15 h was chosen as the relative equilibrium time for each experiment.

## 3 Results and discussion

The rectangular piers with different  $L/b$  ratios in flow direction ( $\alpha = 0$ ) were positioned at  $60, 90$  and  $120^\circ$  of the bend for scour pattern experiments. The main goal was to determine the minimum amount of  $K_L$ . The amount of  $K_L$  is found when the maximum scouring depth at the pier nose is divided by the maximum scouring depth of the pier at  $L/b = 1$  in each position. All of the conducted experiments and the measuring parameters can be seen in Table 1. In this table,  $d_{sm}$  is the depth of the scouring hole,  $A$  and  $V$  are, respectively, the area and volume of the scouring hole,  $h_{sm}$  is the maximum height of sedimentation,  $y$  is the flow depth at the beginning of the bend,  $B$  is the channel width,  $b'$  is the distance from the maximum scour depth location or the maximum sedimentation location at the bend to the inner bank which is variable, and  $\theta$  is the positioning angle in the channel from the beginning of the bend. According to the table, in the position of  $60^\circ$  of the bend with an increasing pier length, the maximum scour depth at the piers nose is increasing relative to the located pier with  $L/b = 1$  in this position (P160 experiment). This increased scour depth continues until the P560 experiment. The maximum scour depth near the pier nose has been reduced in the P660 experiment so that the  $K_L$  value in this experiment is 0.87. This was caused due to the pier being installed at the  $60^\circ$  angle of the bend and owing to the long pier length, which acted as a barrier against the secondary flows. Since sedimentary stacks caused by the secondary flows are found in the sharp bends near the outer bank and at the  $50\text{--}70^\circ$  angles of the bend itself, 6 times the pier length causes the bed sediments

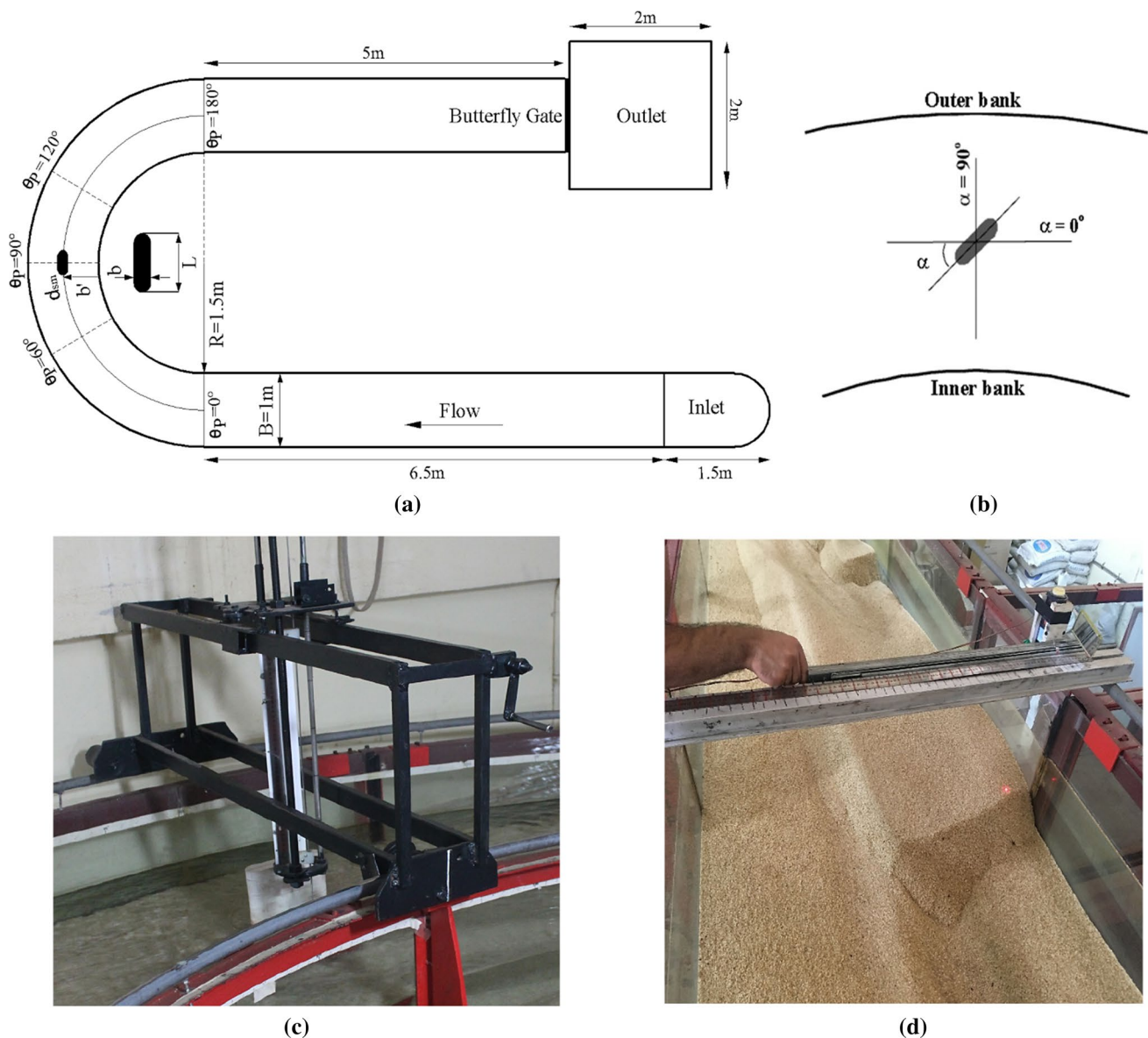


**Fig. 1** Schematic view of (a) laboratory channel and (b) the skewedness angle of pier, (c) temporal variations and (d) bed topography harvesting devices

to be washed off the outer bank and, as a result, the washed sediments along the outer bank and the pier upstream are transferred to the scour hole around the pier and cause the scour hole to be filled around the pier. At the pier position at the angles of  $90^\circ$  and  $120^\circ$ , depending on the curvature relative radius of the bend, sedimentation near the outer bank in the bend without piers is insignificant and the quantitative sediments are introduced from the outer bank to the local scour hole around the pier. Consequently, at the position of  $60^\circ$ , the value of  $K_L$  decreased in comparison with those at two positions of  $90^\circ$  and  $120^\circ$ . With installation of the piers at the position of  $90^\circ$  of the bend, the increase in pier length increases the maximum scour depth at the pier nose. Hence,

the highest amount of the maximum scouring depth is seen in P690 experiment and equals  $1.04y$ . At this point, the coefficient of  $K_L$  reaches 1.21. In addition, with installation of the piers at the position of  $90^\circ$  of the bend, the amounts of the maximum scouring depth at the pier nose are greater than those at the two positions of  $60^\circ$  and  $120^\circ$  of the bend. The volume of scour hole around the piers in Experiments P290 and P390 decreases and then increases by increasing the pier length relative to the volume of the scour hole created in the P190 experiment. What must be taken into consideration is that the volume of the scouring holes developed around the piers at the position of  $90^\circ$  has decreased in comparison with that at the position of  $60^\circ$ . The highest and the

**Table 1** A summary of the measured parameters

| Test No | Identity code | Piers |            | Scour hole parameters |         |         | Position of $d_{sm}$ |        | Position of $h_{sm}$ |          |        | Length factor $K_L$ |
|---------|---------------|-------|------------|-----------------------|---------|---------|----------------------|--------|----------------------|----------|--------|---------------------|
|         |               | $L/b$ | $\theta_p$ | $d_{sm}/y$            | $V/b^3$ | $A/b^2$ | $\theta$             | $b'/B$ | $h_{sm}/y$           | $\theta$ | $b'/B$ |                     |
|         |               | deg   |            |                       |         |         |                      | deg    | %                    | deg      | %      |                     |
| 1       | P160          | 1     | 60         | 0.87                  | 141.3   | 194     | 60                   | 47.5   | 0.58                 | 110      | 5      | 1                   |
| 2       | P260          | 2     | 60         | 0.88                  | 132.8   | 211.7   | 58.5                 | 50     | 0.57                 | 110      | 2.5    | 1                   |
| 3       | P360          | 3     | 60         | 0.89                  | 147.3   | 221.5   | 57.5                 | 52.5   | 0.53                 | 120      | 2.5    | 1.01                |
| 4       | P460          | 4     | 60         | 0.92                  | 175.5   | 235.2   | 57                   | 50     | 0.51                 | 125      | 5      | 1.06                |
| 5       | P560          | 5     | 60         | 0.95                  | 209     | 254.4   | 56.5                 | 52.5   | 0.62                 | 123      | 2.5    | 1.08                |
| 6       | P660          | 6     | 60         | 0.76                  | 201.3   | 290     | 55.5                 | 50     | 0.65                 | 128      | 2.5    | 0.87                |
| 7       | P190          | 1     | 90         | 0.85                  | 137.7   | 177.5   | 89                   | 50     | 0.55                 | 165      | 12.5   | 1                   |
| 8       | P290          | 2     | 90         | 0.89                  | 91.4    | 155.3   | 88.5                 | 50     | 0.51                 | 135      | 10     | 1.04                |
| 9       | P390          | 3     | 90         | 0.9                   | 117.4   | 161.2   | 87.5                 | 52.5   | 0.47                 | 130      | 17.5   | 1.06                |
| 10      | P490          | 4     | 90         | 0.92                  | 148.8   | 180.5   | 87                   | 50     | 0.48                 | 135      | 17.5   | 1.08                |
| 11      | P590          | 5     | 90         | 1.02                  | 173.6   | 203.3   | 86                   | 50     | 0.49                 | 136      | 15     | 1.19                |
| 12      | P690          | 6     | 90         | 1.04                  | 172     | 205     | 85.5                 | 52.5   | 0.47                 | 135      | 12.5   | 1.21                |
| 13      | P1120         | 1     | 120        | 0.74                  | 64.6    | 99.6    | 119                  | 50     | 0.37                 | 170      | 5      | 1                   |
| 14      | P2120         | 2     | 120        | 0.72                  | 47.7    | 80.6    | 118.5                | 52.5   | 0.31                 | 165      | 7.5    | 0.97                |
| 15      | P3120         | 3     | 120        | 0.82                  | 67.8    | 97.2    | 117.5                | 55     | 0.36                 | 165      | 7.5    | 1.1                 |
| 16      | P4120         | 4     | 120        | 0.85                  | 82      | 118     | 117                  | 47.5   | 0.4                  | 150      | 12.5   | 1.15                |
| 17      | P5120         | 5     | 120        | 0.93                  | 98.4    | 158.3   | 116.5                | 52.5   | 0.38                 | 150      | 5      | 1.25                |
| 18      | P6120         | 6     | 120        | 0.91                  | 99.3    | 132.5   | 115.5                | 52.5   | 0.4                  | 149      | 10     | 1.22                |

lowest amounts of the maximum scouring depth at the pier nose with  $L/b = 1$  occurred at the position of 60 and 120° of the bend, respectively. In the piers with length-to-width ratios of 2 to 6, the maximum and the minimum depth of scouring at the pier nose, respectively, occurred at the position of 90 and 120° of the bend. Also, the maximum scour depth at the pier nose has increased at the position of 120° of the bend by increasing the pier length. The maximum area of the scour hole created around the piers occurred in the P660 experiment and was equal to 290  $b^2$ . It is also the lowest in the P2120 experiment and was equal to 80.6  $b^2$ . The volume of the scour hole developed around the pier at the position of 60° was higher than that found at positions of 90 and 120°. The maximum and the minimum volumes of the scouring hole were, respectively, found in Experiments P560 and P2120 and were equal to 209  $b^3$  and 47.7  $b^3$  around the piers. In each position, with an increase in pier length, the coefficient of  $K_L$  is also increasing. The amounts of  $K_L$  coefficient at the position of 120° are higher than those at the position of 90°, and both are higher than those at the position of 60°. The maximum coefficient of  $K_L$  was found in P5120 experiment and its minimum amount was found in P660 experiment, each, respectively, at 1.25 and 0.85.

A sample of scouring contours which were found around the pier at the position of 90° from the bend has been depicted in Fig. 2. It can be seen that increasing the pier length leads to an increase in the width of the scouring hole near the pier nose, and when it moves downstream,

this width decreases. This is because the pier length has inhibited the secondary flow development. The secondary flow generated in the bend is diverted towards the outer bank and oriented towards the bed due to collision with the pier length. Therefore, it causes scour around the pier nose. It also results in the scour hole orientation towards the inner bank at the downstream side of the pier so that increasing the pier length further orients the scour hole towards the inner bank. With an increase in the pier length, the length of the scouring hole at the upstream side of the pier nose increases while moving upstream. This is all true while the opposite takes place downstream of the piers, i.e., an increase in the pier length leads to a decrease in the length of the scouring hole formed at the downstream side of the pier. Based on Fig. 2a, the scouring hole caused around the pier has started from 6b towards upstream and continued towards 14b downstream of the pier as shown in P190 experiment. Hence, the sediments extracted from the scouring hole from the 130 to 170° angles from the bend have been stacked at 28b and 55b amounts across the inner bank. Additionally, these sediments have gone into a straight downstream path and continue to move downstream until they reach 6b from the end of the bend. Based on P290 experiment in Fig. 2b, the scouring hole has been formed at 6b towards upstream of the pier and 10.5b towards its downstream side. The accumulated sediments resulting from this scouring were observed between the angles of 120 and 145° from the bend and, respectively, equal 21b and 38b towards the pier

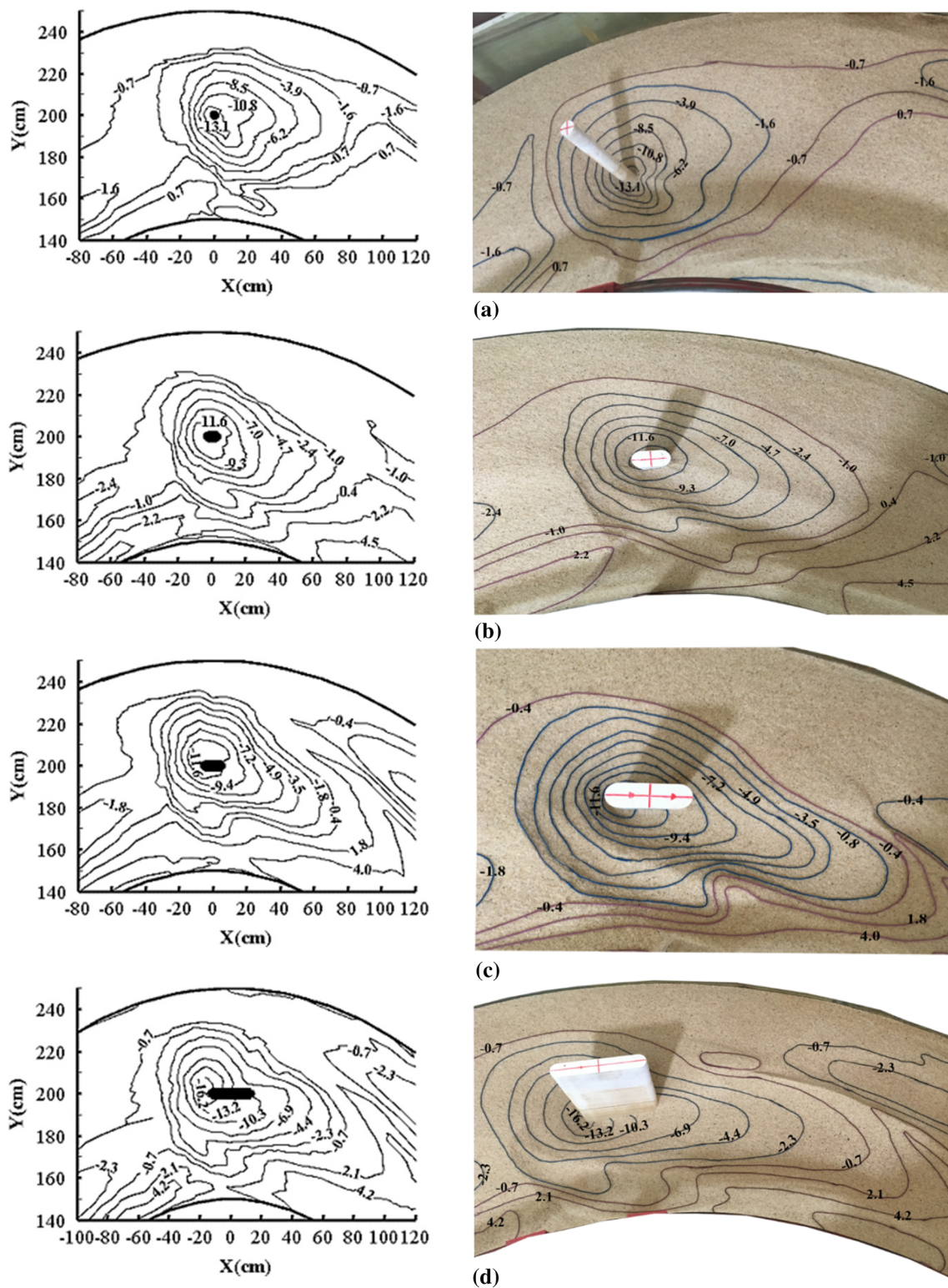


**Fig. 2** Samples of scour contours in experiment (a) P190, (b) P290, (c) P390 and (d) P690

downstream and a distance of  $0.45B$  from the inner bank. According to Fig. 2c, the scouring hole in P390 experiment is formed between angles of  $80$  and  $115^\circ$  from the bend

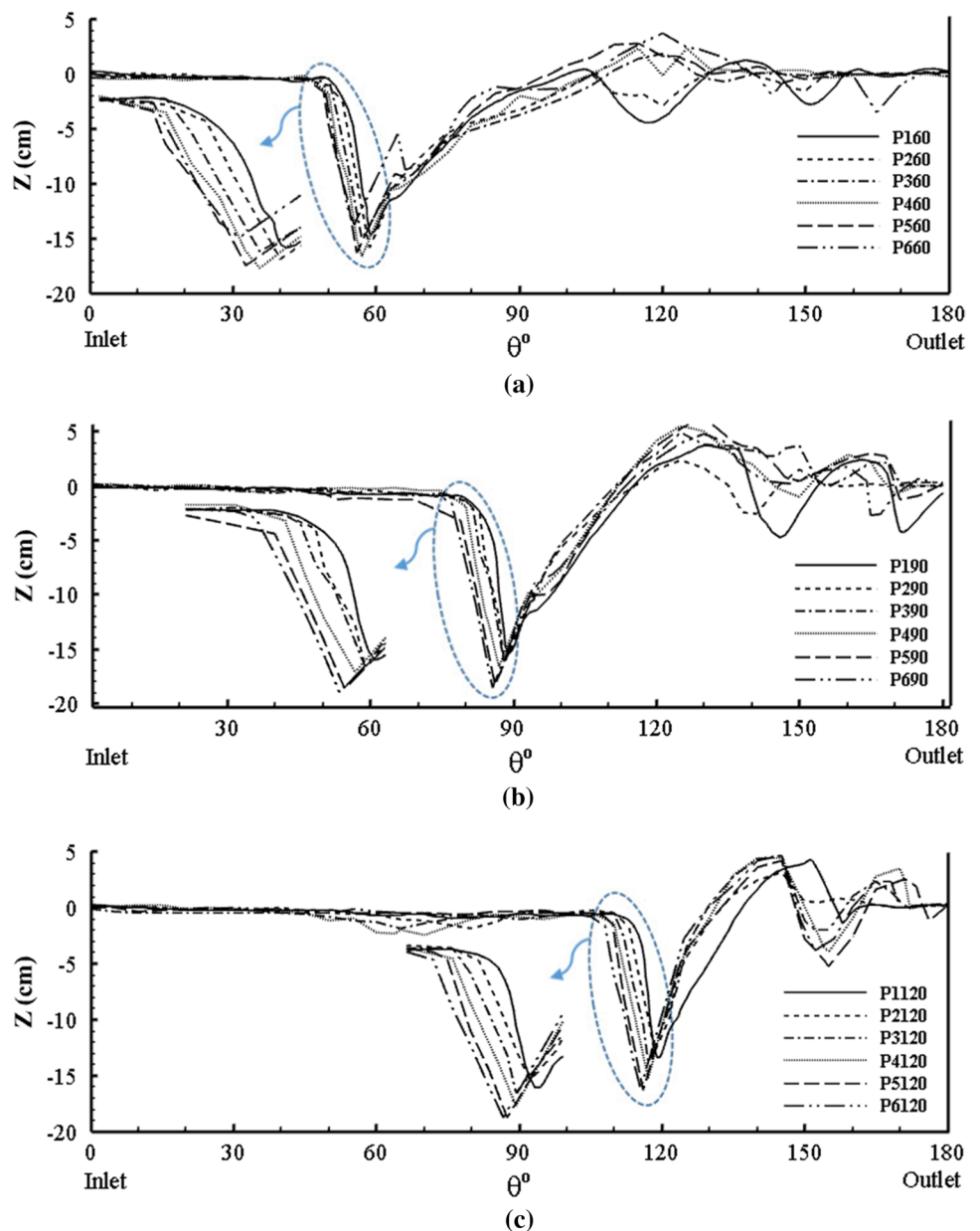
and, respectively, equal  $6b$  and  $17b$  towards the upstream and downstream sides of the pier. In addition, the sediments extracted from the scouring hole at  $120$ – $150^\circ$  angles equal

21*b* and 40*b* pier downstream and have been stacked at 0 to 0.5*B* from the inner bank. As can be seen in Fig. 2d, in contrast to previous three experiments, the scouring hole in P690 experiment has started from the angle of 70° equal to 10.5*b* from the pier upstream and has continuously moved towards the angle of 115° equals to 17*b* to the pier downstream. The sediments washed away from the vicinity of the pier have been stacked at 120–155° angles from the bend due to horseshoe and wake vortices near the inner bank of the pier downstream. Also, the sediments near the inner bank have continuously formed up to 6*b* from the bend towards a straight path in downstream direction.

Figure 3 illustrates a sample of bed length profiles located at a 50% distance of the channel width from the inner bank

in different situations. *Z* is the distance from the initial bed level. The volume of sediments leaving the scour hole around the piers is increased when the piers are installed at the first half of the bend in comparison with the case where they are located in the second half of the bend due to the influence of the upstream straight path and the high power of wake vortices. In Fig. 3a, where the piers are located at the position of 60° from the bend in the length profile from the centre of the channel, the bed characteristics are similar from the beginning to an angle of about 50° for all piers. The bed changes found in all experiments were pretty similar from an angle of 50° equal to 10*b* towards upstream to nearly an angle of 110° equal to 35*b* downstream. These changes occur in a trend that the length of the scour holes

**Fig. 3** Samples of longitudinal sections at positions of (a) 60, (b) 90 and (c) 120° with zoomed areas around the piers





upstream of the piers nose increases with an increase in the pier length, as shown in the zoomed area. However, at the downstream side of the pier tail, an increase in the pier length decreases the length and depth of the scour holes downstream. In addition to an increase in the power of the secondary flow, the depth of the scouring holes at the pier location have also reached its maximum amount. Sedimentary deposits have been formed at an angle of  $110^\circ$  equal to  $35b$  pier downstream to an angle of  $140^\circ$  equal to  $55b$  pier downstream, except in Experiments P160 and P260. In these two experiments, the scour around the piers is lower due to the small pier length; therefore, less sediment is carried downstream, and the water falling from the sedimentary stacks on the bed results in generation of scour holes in the stated periods. An increase in the pier length leads to an increase in the height of the sedimentary stacks. Hence, the maximum height of sedimentation of  $0.3y$  was found at the angle of  $120^\circ$  in P660 experiment. Except for P660 experiment, no significant changes were found in the bed topography of the remaining experiments from an angle of  $160^\circ$  to the end of the bend. According to Fig. 3b, by placing the pier at the  $90^\circ$  angle, no significant changes are observed from the beginning to the angle of  $65^\circ$  from the bend, and the bed in all experiments is approximately at its initial level. Also, from the range of  $70$ – $110^\circ$  around the pier, a scour hole has been created; with an increase in the pier length, the depth and length of scour holes increase. The sediments carried from the scouring hole piled up around the piers from the

$110$  to  $140^\circ$ . The highest amount of sediments, which was  $0.4y$ , was found in P590 experiment and the lowest amount,  $0.15y$ , was found in P290 experiment. From the angle of  $140^\circ$  to the end of the bend, scouring and sedimentation are repeated alternately. In Fig. 3c, by placing the piers at the position of  $120^\circ$  from the bend, similar to Fig. 3a, an increase in the pier length will lead to an increase in the length and depth of the scouring hole in the pier upstream and a decrease in the pier downstream. The scouring holes have been formed around the piers from the angle of  $110^\circ$  equal to  $10b$  the pier upstream to approximately the angle of  $140^\circ$  equal to  $14b$  towards downstream. The sediments leaving the scouring hole have been piled up from the angle of  $115$ – $150^\circ$  in rectangular piers, while in P1120 experiment, from the angle of  $140$ – $160^\circ$ , a sedimentary stack is formed. The greatest height of sedimentation was found in Experiments P5120 and P4120, both rating at the amount of  $0.3y$  at an angle of  $145^\circ$ . In addition, when water poured down from above the sedimentary stacks onto the bed, scouring holes were created at  $150$ – $160^\circ$  angles and the sediments carried away from the holes were piled up at the  $170^\circ$  angle. No significant changes were found at the end of the bend in the experiments.

In Fig. 4, the maximum amount of dimensionless sedimentation is illustrated with the flow depth at the beginning of the bend against its position along the bend. The  $\theta\pi R/180$  axis is indicative of the longitudinal direction from the beginning to the end of the bend in metres, which has

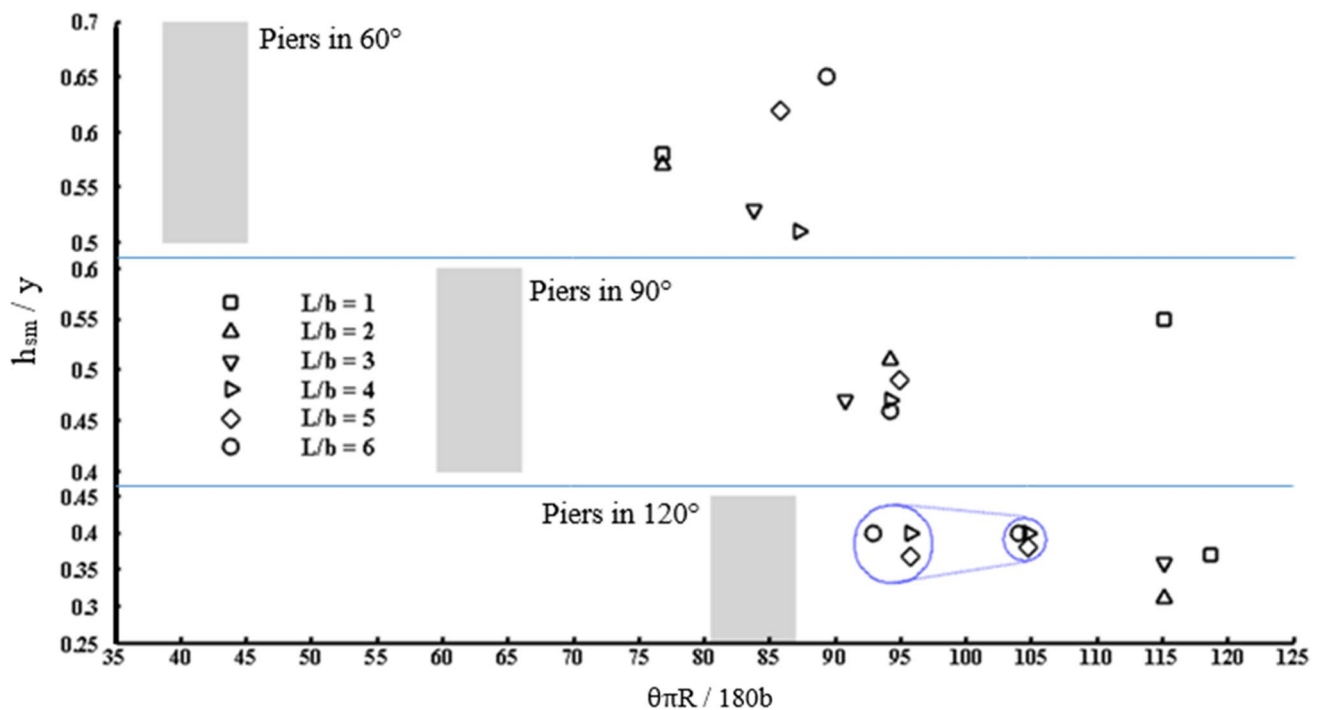


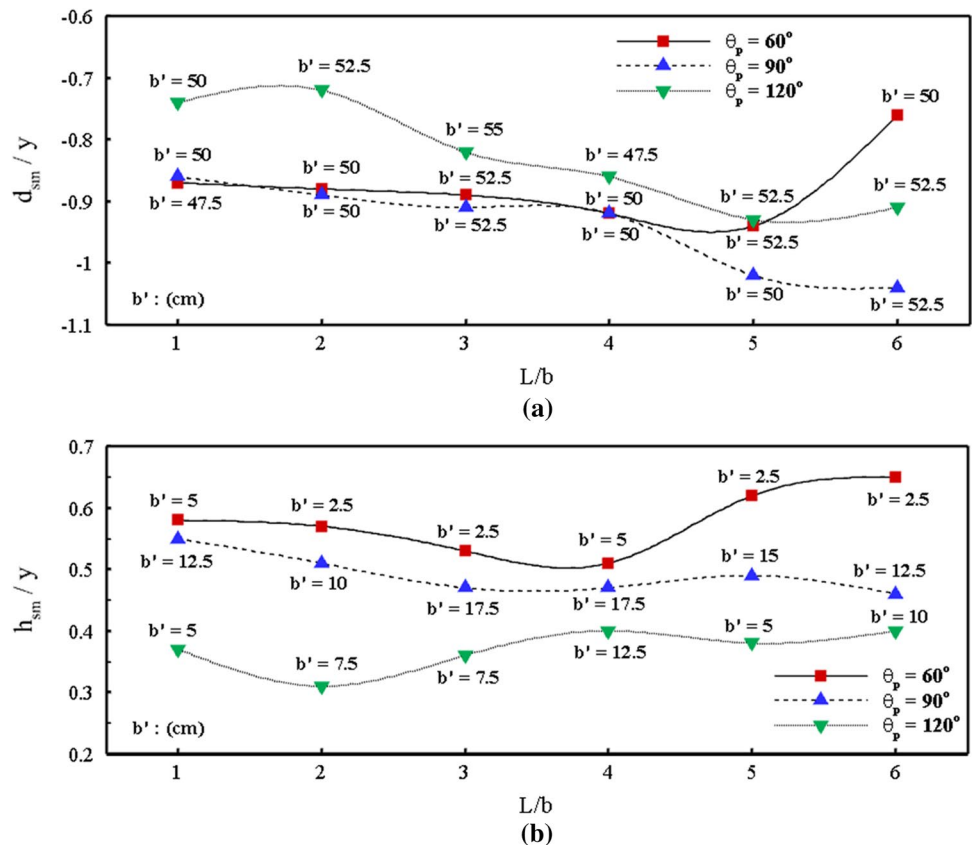
Fig. 4 Position of the maximum sedimentation along the bend

been dimensionless with the pier width. As can be seen in the figure, by placing the piers at the position of  $60^\circ$ , the height of the sediments and their distance from the piers centre are greater than those at the positions of  $90^\circ$  and  $120^\circ$ . In comparison with the second half of the bend, the first half is influenced by the upstream straight path and is also further affected by the downstream bend. Following an increase in the secondary flow power and hence the spiral flow in this half, further development of sediments towards the downstream side of the piers is observed. The maximum height of sedimentation occurs when the pier with  $L/b=6$  is placed at the position of  $60^\circ$  and the lowest amount is found when the pier with  $L/b=2$  is placed at the position of  $120^\circ$ . Also, the maximum and minimum distances from the piers centre occurred by placing the pier with  $L/b=6$  at the positions of  $60$  and  $120^\circ$  of bend, respectively. By placing the piers at the position of  $60^\circ$  from the bend and increasing the pier length, the distance between the maximum sedimentation and the piers centre will increase. The maximum distance is found in the pier with  $L/b=6$  at a  $0.65y$  height placed at a distance of  $50b$  towards downstream. In addition, the lowest distance was found in the piers with  $L/b=1, 2$  which, respectively, had heights of  $0.58y$  and  $0.57y$  and were placed at  $35b$  towards downstream. By placing the piers at the position of  $90^\circ$  in the bend and increasing the pier length, the maximum height of sedimentation decreased. The highest

amount of sedimentation was found in the pier with  $L/b=1$  and the lowest at the pier with  $L/b=6$ . The highest and lowest amounts of sedimentation were, respectively,  $0.55y$  and  $0.46y$ . In this position, the point at which the maximum amount of sedimentation occurred towards the pier centre has been placed at an approximate  $35b$  downstream distance in all the piers. By placing the piers at the position of  $120^\circ$  from the bend, unlike the position of  $90^\circ$ , an increase in the pier length led to an increase in the height of the maximum sedimentation found in the piers downstream. The maximum height of sedimentation was found in the pier with  $L/b=6$  and was  $0.4y$  high, while the minimum height was found in the pier with  $L/b=1$  with a height of  $0.31y$ . In addition, by increasing the pier length in this position, the distance of the maximum sedimentation height from the piers centre has decreased. The maximum and minimum distances, respectively, occur at piers with  $L/b=1, 2$  and  $L/b=6$  at distances of  $30b$  and  $20b$  at the downstream side of the piers.

The locations of the maximum scour depth and sedimentation height, nondimensionalized with the flow depth at the beginning of the bend, are shown in Fig. 5 against different positions along the channel width from the inner bank. The maximum scour depth, with the placement of piers in different positions, occurred near the piers nose. It can be seen from Fig. 5a that by placing the piers at the positions of  $60, 90$  and  $120^\circ$  from the bend, the variation range of the

Fig. 5 Location of the maximum (a) scour depth and (b) sedimentation height on the channel width

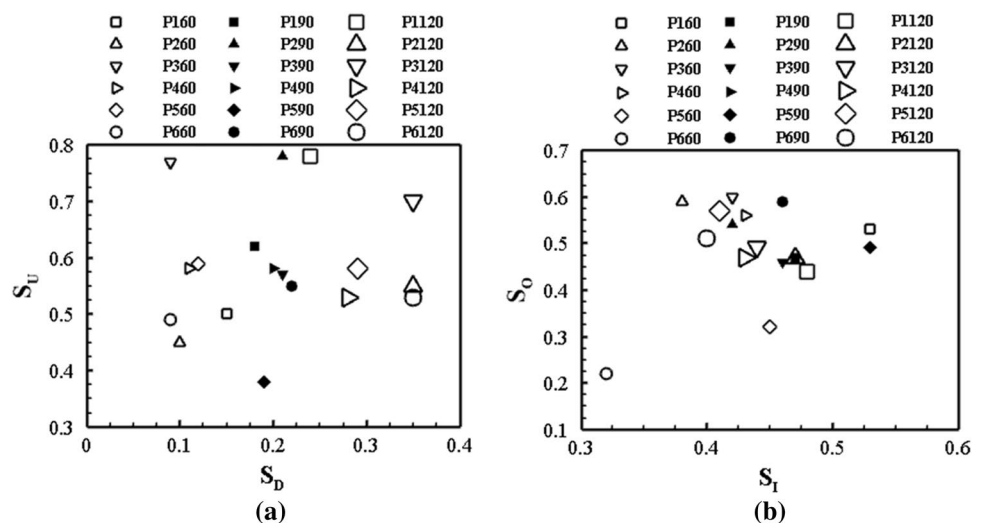


maximum scour depth occurred at 50–52.5, 47.5–52.5 and 47.5–55% of the channel width from the inner bank, respectively, due to the flow crash in the first encounter with the pier on the nose and the presence of downflow. By placing the piers at the positions of 90 and 120° from the bend, the maximum and minimum scour depths, respectively, occur near the pier nose. The maximum amount of scouring occurs near the nose of the pier with  $L/b=6$ , equal to  $1.04y$ , at the position of 90°, and its minimum amount is found in front of the pier nose with  $L/b=2$ , equal to  $0.72y$ , at the position of 120° in the front of the pier nose. As it can be seen in Fig. 5b, the location of the maximum height of sedimentation in the channel width for different piers at the positions of 60, 90 and 120° from the bend have, respectively, occurred at intervals of 2.5–5, 10–17.5 and 5–12% of the channel width from the inner bank. The sediment leaving the scour hole and moving downstream reaches an area where the pier influence is reduced. Therefore, once again it undergoes the influence of the secondary flow generated in the bend and orients towards the inner bank. As a result, the maximum sedimentary height occurs near the inner bank. The maximum height of sedimentation increases by placing the piers at the 60° angle in comparison with the 90° one, with both angles showing more increase in comparison with the 120° angle. This is due to approximation to the downstream straight path and a reduction in the vortices power, including the wake vortices. The maximum height of sedimentation is formed at the 60° angle and  $0.025B$  from the inner bank, and the lowest height of sedimentation is formed at  $0.075B$  from the inner bank, respectively, at the downstream side of the piers with  $L/b=6$  and  $L/b=2$ . Also, the maximum and minimum heights of sedimentation, respectively, fall at  $0.65y$  and  $0.31y$ .

The slopes of the walls around the scour holes formed around the rectangular piers in different positions have been depicted in Fig. 6. In this figure,  $S_D$  and  $S_U$ , respectively,

represent the slope of the upstream and downstream walls and  $S_I$  and  $S_O$ , respectively, denote the slope of the wall towards the inner and outer banks of the scouring hole. In order to determine the slope of the scour hole walls in different directions, first the location and the amount of the maximum scour hole depth was specified. Then the angle between the oblique and straight lines from the location of the maximum scour depth to the hole side walls, which is in fact the slope on the sides of the scour hole wall, was calculated. Based on Fig. 6a, the amount of  $S_D$  increases when the piers are placed at the position of 120° in comparison with the position of 90°, and both positions show higher levels of increase in comparison with the position of 60°. When the scour hole occurs in the second half of the bend, the progress of scour hole towards the downstream side of the piers is less than that in the first half. Hence, a reduction in the horizontal distance between the downstream wall of the scour hole and the location of the maximum scour depth leads to an increase in the downstream wall slope. The maximum amount of  $S_D$  is 0.35, found in all the three Experiments of P2120, P3120 and P6120. The amount of  $S_U$  in P3120 experiment was 0.7, which is higher in comparison with the other two experiments. In addition, the lowest amount of  $S_D$  is 0.09 in both Experiments P360 and P660. However, the amount of  $S_U$  is 1.5 times higher in P360 experiment than that in P660 experiment. The maximum amount of  $S_U$  in Experiments P290 and P1120 is 0.78, and the minimum amount in P590 experiment is 0.38. As it can be seen in Fig. 6b, the minimum amounts of  $S_I$  and  $S_O$  occurred in P660 experiment, respectively, amounting to 0.32 and 0.22. This was caused by the high width of the scour hole created around the pier in this experiment; a scour hole occupied 85% of the channel width itself. The maximum amount of  $S_O$  was found in P360 experiment at 0.6. Also, the maximum amount of  $S_I$  in both Experiments P160 and P590 was 0.53. One of the important points that must be considered is

**Fig. 6** Wall slope of (a) upstream and downstream and (b) the inner and outer banks of the scour holes around the pier in different positions



that in Experiments P160, P190, P390, P490 and P2120, the slope of the inner and outer bank walls is the same, proving that the maximum depth of scouring is found in the middle of the scour hole width in these experiments. In addition, the higher amount of  $S_I$  in comparison with  $S_O$  shows that the scour hole is more likely to move towards the outer bank and vice versa.

Given that placing the rectangular pier with  $L/b=6$  along the bend channel can lead to scouring and destruction of the inner bank, using it in a  $180^\circ$  sharp bend is not advised. Additionally, Melville and Sutherland’s study in 1988 investigating the length-to-width ratio of the rectangular pier in the straight channel proved that the length of the rectangular pier in such studies must be 3 times the width ( $L/b > 2$ ) [38]. Based on the obtained results of the present study regarding the relationship between the length and width at a  $180^\circ$  sharp bend and its comparison with Melville and Sutherland’s study [38], it can be concluded that it is best to use rectangular piers with a length-to-width ratio of 3–5 ( $3 \leq L/b \leq 5$ ) in a  $180^\circ$  sharp bend in order to prevent the destruction of the banks and cause less alterations to the topography of the bed. The performance of the rectangular pier with a length-to-width ratio of 3, positioned at 60, 90 and  $120^\circ$  of the bend, in terms of the volume of the scour hole formed around the pier, the length and width of the scour hole, the maximum scour depth in front of the pier nose, and the bed topography changes in the pier downstream, according to Table 1, is better than the performance of the two rectangular piers with  $L/b = 4, 5$ . Hence, utilizing this rectangular pier at different positions of a  $180^\circ$  bend leads to better results. Given that a pier with  $L/b = 3$  can decrease the scouring of the bend more efficiently, and that the maximum depth of the scouring around the pier in a  $90^\circ$  position is higher in comparison with the other positions, the skewness of the pier parameter

with different angles of attack towards the inner and outer banks with a ratio of  $L/b = 3$  was investigated.

In Table 2, the coefficient of  $K_\alpha$  is defined for the maximum scour depth created around the skewed pier with different collision angles of the flow. This coefficient is obtained by dividing the maximum scour depth created around the skewed pier with different collision angles of the flow to the pier by the maximum scour depth created around the pier when it is longitudinal to the flow direction. In Table 2,  $\alpha$  is the skewness angle of the skewed pier towards the banks and  $L_D$  is the sediments progress in the straight downstream path. By placing the skewed pier towards the inner bank, the maximum scour depth in Experiment  $P + 60$  with a skewness angle of  $\alpha = 60^\circ$  equals  $1.51y$ . By moving the angle towards the outer bank, the maximum scour depth was recorded to be  $\alpha = -75^\circ$  and equals  $1.22y$ . When the pier is skewed towards the inner bank, an increase in  $\alpha$  leads to an increase in  $K_\alpha$ . This is the case while by increasing  $\alpha$  by skewing the pier towards the outer bank, the  $K_\alpha$  coefficient only increases at the pier with  $\alpha \geq 45^\circ$ , and in the pier with  $\alpha < 45^\circ$ , the amount of this coefficient is smaller than one. By skewing the pier with angles of 15 and  $30^\circ$  to the outer bank, the maximum scour depth created around the pier would be less than the maximum scour depth when the pier is longitudinal to the flow direction. In the pier with  $\alpha = -15^\circ$ , the maximum scour depth near the pier nose is reduced by about 20% relative to the pier with  $\alpha = 0^\circ$ . In the pier with  $\alpha = 90^\circ$ , the pier is completely perpendicular to the flow; the maximum scour depth around the pier increases by about 55% in comparison with a pier with  $\alpha = 0^\circ$  or, in other words, the coefficient  $K$  is 1.55 times higher. In general, the maximum scour depth when the pier was skewed towards the inner bank was greater than that with skewing it towards the outer bank, and the highest scouring occurred at the highest angle. The

**Table 2** Scouring parameters for skewed rectangular pier

| Test No | Identity code | Piers          |    | Scour hole parameters |         |         | position of $d_{sm}$ |        | position of $h_{sm}$ |          |        | Skewed factor $K_\alpha$ |         |
|---------|---------------|----------------|----|-----------------------|---------|---------|----------------------|--------|----------------------|----------|--------|--------------------------|---------|
|         |               | $\alpha$ (deg) |    | $d_{sm}/y$            | $V/b^3$ | $A/b^2$ | $\theta$             | $b'/B$ | $h_{sm}/y$           | $\theta$ | $b'/B$ |                          | $L_D/b$ |
|         |               | +              | -  |                       |         |         |                      |        |                      |          |        |                          |         |
| 1       | P390          | 0              | 0  | 0.91                  | 117.4   | 161.2   | 87.5                 | 52.5   | 0.47                 | 136      | 17.5   | -                        | 1       |
| 2       | P+15          | 15             | -  | 1.11                  | 202.4   | 231.2   | 88                   | 52.5   | 0.7                  | 163      | 17.5   | 42                       | 1.27    |
| 3       | P+30          | 30             | -  | 1.18                  | 268.9   | 296.7   | 88                   | 52.5   | 0.6                  | 165      | 20     | 74                       | 1.3     |
| 4       | P+45          | 45             | -  | 1.33                  | 321.7   | 301.3   | 88                   | 52.5   | 0.68                 | 165      | 12.5   | 70                       | 1.47    |
| 5       | P+60          | 60             | -  | 1.51                  | 446.1   | 370.6   | 88                   | 55     | 0.74                 | 177      | 30     | 78                       | 1.67    |
| 6       | P+75          | 75             | -  | 1.38                  | 378.6   | 331.7   | 90                   | 57.5   | 0.69                 | 170      | 20     | 66                       | 1.53    |
| 7       | P-15          | -              | 15 | 0.74                  | 92.3    | 147.8   | 88                   | 55     | 0.46                 | 135      | 2.5    | -                        | 0.82    |
| 8       | P-30          | -              | 30 | 0.9                   | 162.9   | 207.7   | 90                   | 47.5   | 0.55                 | 140      | 2.5    | 4                        | 0.99    |
| 9       | P-45          | -              | 45 | 1.08                  | 275.1   | 276.6   | 92                   | 45     | 0.68                 | 172      | 25     | 62                       | 1.19    |
| 10      | P-60          | -              | 60 | 1.16                  | 331.1   | 315.2   | 90                   | 47.5   | 0.69                 | 141      | 12.5   | 70                       | 1.29    |
| 11      | P-75          | -              | 75 | 1.22                  | 369.2   | 361.4   | 89                   | 57.5   | 0.67                 | 140      | 12.5   | 80                       | 1.35    |
| 12      | P90           | 90             | 90 | 1.4                   | 430.6   | 356.5   | 89                   | 60     | 0.69                 | 150      | 12.5   | 80                       | 1.55    |

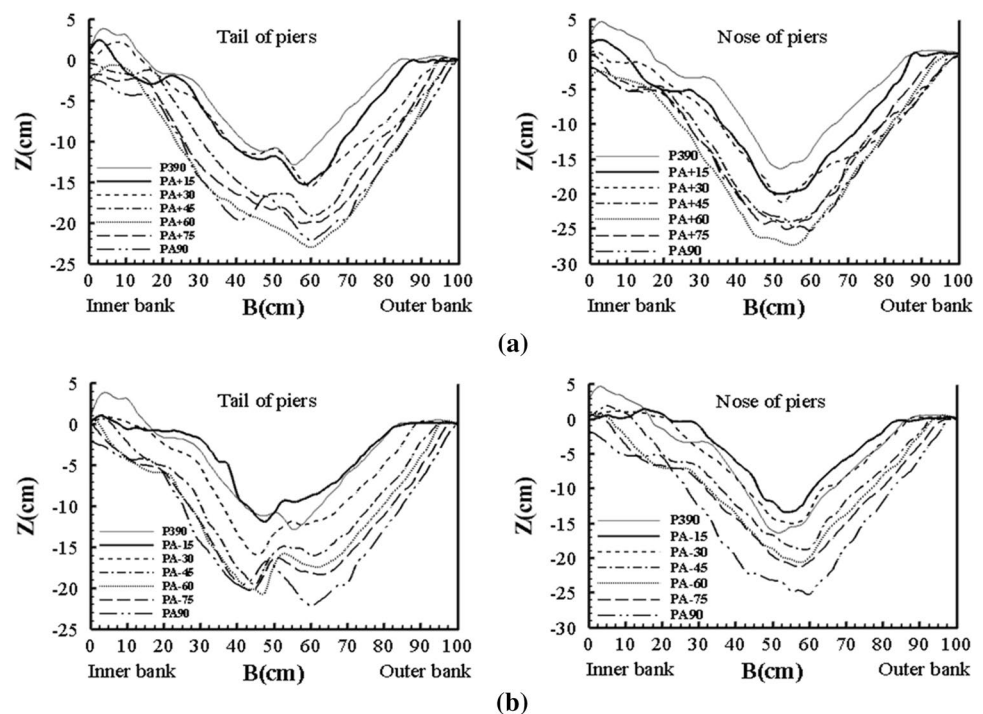
volume of the scouring hole created around the skewed pier is directly linked to an increase in the skewness angles of the pier towards the banks. By increasing  $\alpha$ , the volume of the scour hole has increased in every state, with the exception of the pier with  $\alpha = -15^\circ$ . The maximum volume of the scour hole is, respectively,  $446.1b^3$  and  $369.2b^3$  when the pier is skewed towards the inner bank with  $\alpha = 60^\circ$  and towards the outer bank with  $\alpha = -75^\circ$ . The volume of the scour hole created around the pier with  $\alpha = 90^\circ$  is approximately 3.5 times the volume of the scour hole around the pier with  $\alpha = 0^\circ$ . By skewing the pier towards the banks and due to an increase in  $\alpha$  owing to the increase in cross-sectional area against the flow, it increases the length and width of the scour hole. As a result, the area of the scour hole created around the pier increases with an increase in  $\alpha$ . The maximum lengths of the scour hole in the pier with  $\alpha = \pm 30^\circ$  are, respectively,  $21b$  and  $22.5b$ , and the maximum widths of the scour hole in the piers with  $\alpha = 60^\circ$  and  $\alpha = -75^\circ$  are, respectively, calculated to be  $92.5B$  and  $0.9B$ . Therefore, the maximum area of the scour hole is found around the piers with  $\alpha = 60^\circ$  and  $\alpha = -75^\circ$  and is calculated to be  $370.6b^2$  and  $361.4b^2$ . Skewing the pier towards the banks leads to further progress of the sediment in the straight downstream path, and with the increase in  $\alpha$ , the length of sediment reach increases. The maximum progression of the sediments in the straight downstream path occurs at the piers with  $\alpha = 60^\circ$  and  $\alpha = 90^\circ$  and in both, it is calculated to be  $80b$  from the end of the bend.

A sample of cross sections near the nose and tail of the skewed pier with different skewness angles towards the inner and outer banks has been depicted in Fig. 7. Skewing the

pier towards the inner and outer banks due to placing the piers against and aligned with the secondary flows, respectively, leads to scouring at the banks near the nose and tail of the pier. Therefore, the width of the scour hole increases with an increase in the skewness angle. Also, increasing the width of the scour hole to the inner bank causes the sediment stacks to be washed away in this place. Hence, with skewness angles higher than  $30^\circ$ , sedimentary stacks are not formed near the inner bank in front of the nose and tail of the pier. In Fig. 7a, the maximum width of the scour hole near the pier nose occurred in Experiment  $P+60$  and  $0.925B$ , and that near the pier tail in Experiment  $P90$  and  $0.9B$ . The maximum scour depth in front of the pier tail is estimated in Experiment  $P+60$  to be equal to  $1.49y$  and  $0.6B$  from the inner bank. Based on Fig. 7b, by skewing the pier towards the outer bank in Experiments  $P-15$  and  $P-30$  in front of the pier nose, the maximum scour depth, about 20% and 8%, and the width of the scour holes, about 25% and 8%, respectively, have decreased compared to Experiment  $P390$ . In experiments where  $\alpha \geq 45^\circ$ , by increasing the skewness angle towards the outer bank, the width of the scour hole in front of the nose and tail of the pier increases. In Experiment  $P90$ , due to installation of the pier transverse to the flow direction, the maximum width of the scour hole around the pier is about 55% higher than the pier longitudinal to the flow direction.

A sample of the development of the scour hole to the downstream side of the skewed pier with different angles of skewness towards the inner and outer banks is shown in Fig. 8. In the figures, the location of the maximum scour

**Fig. 7** Cross sections near the nose and tail of the skewed rectangular pier towards the (a) inner and (b) outer banks



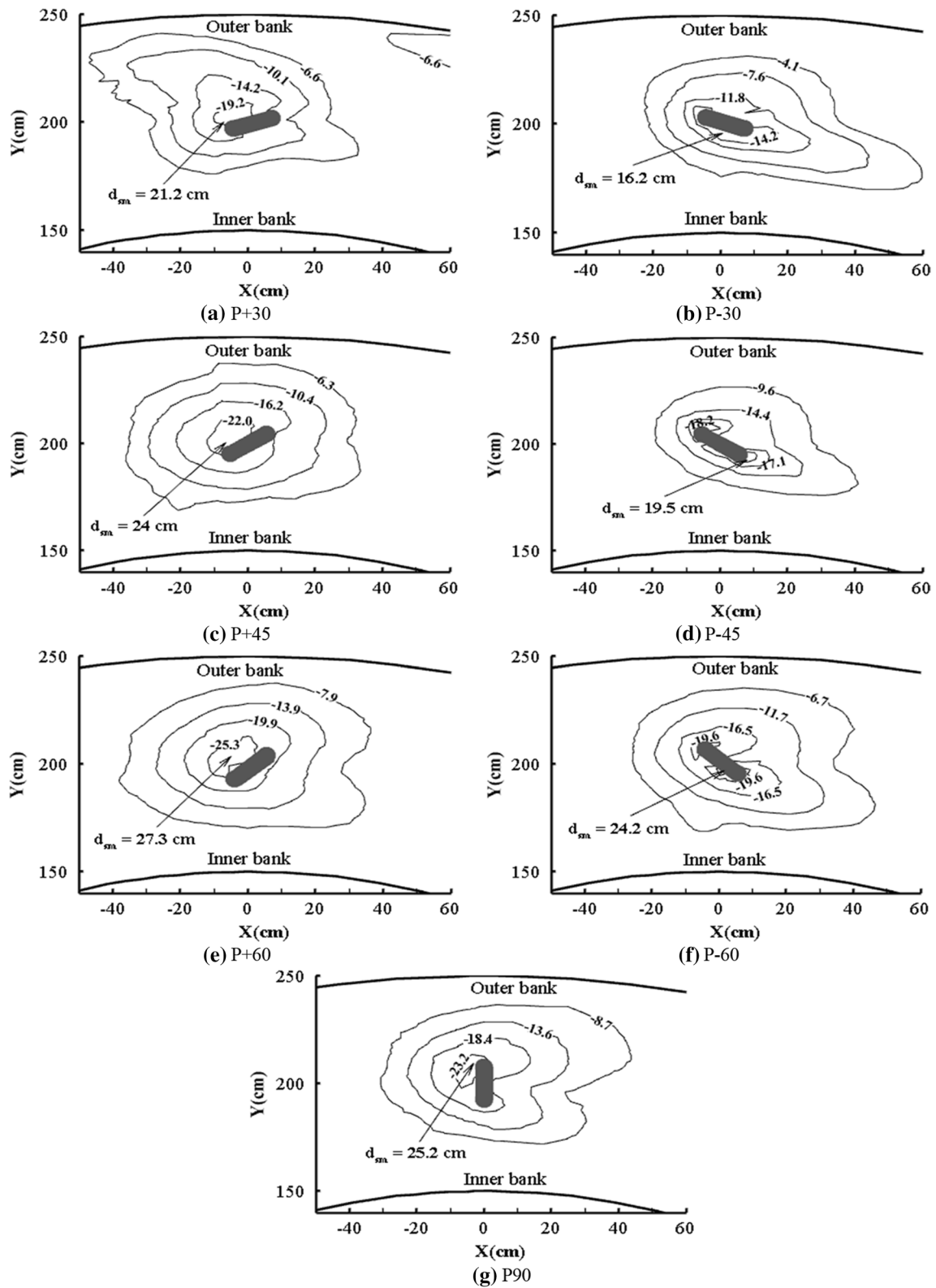
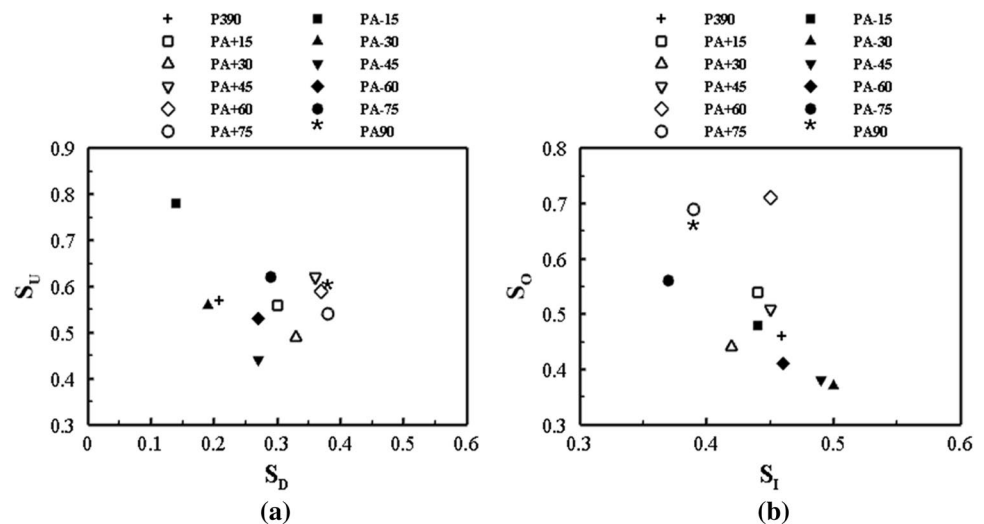


Fig. 8 A sample of the development of the scour hole around the skewed pier

**Fig. 9** Wall slope of (a) upstream and downstream and (b) inner and outer banks of the scour hole around the skewed pier



depth around the pier is shown. By skewing the pier with  $15^\circ \leq \alpha \leq 75^\circ$  towards the inner bank, the scour hole was formed at the pier upstream near the pier nose. Then the scour hole is expanded towards the banks and the pier downstream due to placing the pier against the secondary flows and thus increasing the power of the horseshoe vortex at the pier upstream. In Fig. 8a, in a pier with skewness angles of less than  $45^\circ$  towards the inner bank, the pier upstream end prevents the flow more efficiently than the downstream end. For this reason, at smaller angles, the scour hole occurs near the pier nose upstream. Also, in accordance with Fig. 8b, skewing the pier towards the outer bank at an angle of less than  $45^\circ$  causes a scour hole at its downstream end close to the pier tail. Then the scour hole expands towards the downstream side of the pier leaning towards the inner bank. Figure 8c indicates that an increase in the  $\alpha$  angle towards the inner bank not only affects the upstream end of the pier but also has an impact on the downstream end by causing an obstacle in the flow which leads to an increase in the speed and power of the downflows in the upstream pier. As a consequence, the scour hole expands towards the pier downstream end, covering the entire pier length. According to Fig. 8d, two scour holes around the skewed pier, one near the nose and the other near the tail, have been formed in the pier with  $\alpha \geq 45^\circ$  and towards the outer bank. This is due to the pressure gradient at the pier upstream which deviates the downflows near the pier nose towards the two sides of the pier. Hence, by increasing the skewness angle towards the outer bank, the scour holes developed further at the two ends of the pier. Figure 8e shows that an increase in the  $\alpha$  angle towards the inner bank causes the maximum scour depth to occur away from the pier and orient towards the outer bank because most of the pier length is located against the secondary flows. Also, in Fig. 8f, by increasing the skewness angle towards the outer bank, the maximum scour depth location

is moved from the front of the pier nose to the pier tail and closer to the inner bank in comparison with the case where the pier is longitudinal to the flow direction. According to Fig. 8g, with installation of the pier transverse to the flow direction, since the pier end close to the outer bank is located against the secondary flows, a scouring hole is generated near the outer bank and develops towards the downstream side of the pier by orienting in the outer bank direction.

The walls slope of the scour holes formed around the skewed pier with different skewness angles is shown in Fig. 9. As shown in Fig. 9a, skewing the pier towards the bank, and increasing  $\alpha$  leads to an increase in the  $S_D$  amount as well. The  $S_D$  amounts in the skewed pier towards the inner bank are higher than those in the pier skewed towards the outer bank. The skewed pier towards the outer bank increases the scour hole length in downstream direction because of the pier installation longitudinal to the secondary flow. Therefore, the downstream wall slope decreases. However, skewing the pier towards the inner bank leads to the reverse. The highest amount of  $S_D$  occurred in Experiments P+75 and P90, and in both cases, it was 0.38. The lowest amount of  $S_D$  was in Experiment P-15 and was equal to 0.14. With an increase in  $\alpha$  in piers with skewness angles of more than  $45^\circ$  towards the inner and outer banks, the amount of  $S_U$  decreased and increased, respectively. The highest and lowest  $S_U$  amounts occurring in Experiments P-15 and P-45 were calculated at 0.78 and 0.44, respectively. In Fig. 9b, by skewing the pier towards the outer bank,  $S_I$  amounts have increased in comparison with the case where the pier is skewed towards the inner bank. This is the case while  $S_O$  amounts have increased by skewing the pier towards the inner bank. As a result, it can be stated that by skewing the pier towards the banks, the scour hole created around the pier moves towards the opposite bank. By skewing the pier towards the inner bank, the highest amounts of  $S_I$  and  $S_O$

occurred in Experiments P+45 and P+60 ranking at 0.45 and 0.71, respectively. By placing the pier transverse to the flow direction relative to the pier longitudinal to the flow direction, the  $S_1$  amount is reduced by about 15%, and the  $S_O$  amount is increased by about 40%.

## 4 Conclusions

In this paper, the scour formed around the rectangular piers with different ratios of length to width and in three positions of 60, 90 and 120° from the 180° sharp bend was investigated. The effect of skewing the pier with different angles of skewness towards the inner and outer banks and its effects on scouring at the position of 90° of the bend was also investigated. The experimental data analysis and results showed that in a 180° sharp bend, the length-to-width ratio of pier between 3 and 5 could have a good performance in reducing the scour depth. The maximum scour depth and the scour hole width occurred by placing the pier at the position of 90°, while the maximum volume and area of the scour hole created around the piers occurred when the piers were located at the position of 60° from the bend. Also, the minimum depth, volume and area of the scour hole occurred around the piers located at the position of 120°. A rectangular pier with a length-to-width ratio of 3 has a better performance in terms of reducing the scour depth than the rest of the piers located along the bend.

The results obtained from the study of the skewness angle of the pier with a ratio of length to width of 3 positioned at 90° showed that increasing the angle of skewness towards the inner and outer banks resulted in an increase in the scouring parameters (depth, volume, length and width of the scour hole) around the pier. The amounts of scouring parameters increased further with the pier skewing more towards the inner bank than the outer bank. In the skewed pier towards the outer bank with an angle of 15°, the scour depth and volume of scour hole in relation to the pier placement longitudinal to the flow direction are both reduced by about 20%, and in the skewed pier with an angle of 30°, the scour depth at the pier nose is reduced by about 8%.

## References

- Chiew YM, Melville BW (1987) Local scour around bridge piers. *J Hydraul Res* 25(1):15–26. <https://doi.org/10.1080/00221688709499285>
- Dargahi B (1990) Controlling mechanism of local scouring. *J Hydraul Eng* 116(10):1197–1214. [https://doi.org/10.1061/\(asce\)0733-9429\(1990\)116:10\(1197\)](https://doi.org/10.1061/(asce)0733-9429(1990)116:10(1197))
- Kumar V, Ranga Raju KG, Vittal N (1999) Reduction of local scour around bridge piers using slot and collar. *J Hydraul Eng (ASCE)* 125(12):1302–1305. [https://doi.org/10.1061/\(ASCE\)0733-9429](https://doi.org/10.1061/(ASCE)0733-9429)
- Bozkus Z, Yildiz O (2004) Effects of inclination of bridge piers on scouring depth. *J Hydraul Eng* 130(8):827–832. [https://doi.org/10.1061/\(ASCE\)0733-9429\(2004\)130:8\(827\)](https://doi.org/10.1061/(ASCE)0733-9429(2004)130:8(827))
- Sheppard DM, Odeh M, Glasser T (2004) Large scale clear-water local pier scour experiments. *J Hydraul Eng* 130(10):957–963. [https://doi.org/10.1061/\(asce\)0733-9429\(2004\)130:10\(957\)](https://doi.org/10.1061/(asce)0733-9429(2004)130:10(957))
- Zarrati AR, Gholami H, Mashahir MB (2004) Application of collar to control scouring around rectangular bridge piers. *J Hydraul Res* 42(1):97–103. <https://doi.org/10.1080/00221686.2004.9641188>
- Zarrati AR, Nazariha M, Mashahir MB (2006) Reduction of local scour in the vicinity of bridge pier groups using collars and riprap. *J Hydraul Eng* 132(2):154–162. [https://doi.org/10.1061/\(asce\)0733-9429\(2006\)132:2\(154\)](https://doi.org/10.1061/(asce)0733-9429(2006)132:2(154))
- Bozkus Z, Ceceme M (2010) Reduction of scouring depth by using inclined piers. *Can J Civ Eng* 37(12):1621–1630. <https://doi.org/10.1139/L10-099>
- Mashahir MB, Zarrati AR, Mokallaf E (2010) Application of riprap and collar to prevent scouring around rectangular bridge piers. *J Hydraul Eng* 136(3):183–187. [https://doi.org/10.1061/\(asce\)hy.1943-7900.0000145](https://doi.org/10.1061/(asce)hy.1943-7900.0000145)
- Chaudhuri S, Debnath K (2013) Observations on initiation of pier scour and equilibrium scour hole profiles in cohesive sediments. *ISH J Hydraul Eng* 19(1):27–37. <https://doi.org/10.1080/09715010.2012.749011>
- Ismail Z, Jumain M, Sidek F, Wahab AK, Ibrahim Z, Jamal M (2013) Scour investigation around single and two piers side by side arrangement. *Int J Res Eng Technol* 2(10):459–465
- Aghaee-Shalmani Y, Hakimzadeh H (2014) Experimental investigation of scour around semi-conical piers under steady current action. *Eur J Environ Civil Eng* 19(6):717–732. <https://doi.org/10.1080/19648189.2014.968742>
- Ahmad N, Melville B, Mohammad T, Ali F, Yusuf B (2016) Clear-water scour at long skewed bridge piers. *J Chin Inst Eng* 40(1):10–18. <https://doi.org/10.1080/02533839.2016.1259021>
- Fael C, Lança R, Cardoso A (2016) Effect of pier shape and pier alignment on the equilibrium scour depth at single piers. *Int J Sedim Res* 31(3):244–250. <https://doi.org/10.1016/j.ijsrc.2016.04.001>
- Shukur AHK, Obeid ZH (2016) Experimental study of bridge pier shape to minimize local scour. *Int J Civ Eng Technol* 7(1):162–171
- Talib A, Obeid ZH, Ham HK (2016) New imperial equation for local scour around various bridge piers shapes. *Int J Sci Res (IJSR)* 5(9):654–658
- Shukri MT (2017) Experimental study of local scour depth around cylindrical bridge pier. *World Acad Sci Eng Technol Int J Civ Environ Struct Const Archit Eng* 11(1):31–36
- Abozeid G, Darweesh S, M, H Saleh H, (2020) Reduction of local scour around oblong bridge piers using slots. *J Adv Eng Trends* 39(1):45–62
- Ahmed SI, Khassaf SI (2020) Study the local scour around different shapes of non-uniform piers. *Basrah J Eng Sci* 20(1):12–14
- Odgaard AJ, Bergs MA (1988) Flow processes in a curved alluvial channel. *Water Resour Res* 24(1):45–56. <https://doi.org/10.1029/wr024i001p00045>
- Sui J, Fang D, Karney BW (2006) An experimental study into local scour in a channel caused by a 90 bend. *Can J Civ Eng* 33(7):902–911. <https://doi.org/10.1139/106-037>
- Masjedi A, Bejestan MS, Kazemi H (2010) Effects of bridge pier position in a 180 degree flume bend on scour hole depth. *J Appl Sci* 10(8):670–675
- Ben Mohammad Khajeh S, Vaghefi M, Mahmoudi A (2017) The scour pattern around an inclined cylindrical pier in a sharp 180-degree bend: an experimental study. *Int J River Basin Manag* 15(2):207–218. <https://doi.org/10.1080/15715124.2016.1274322>



24. Helmy A, Ali M, Ahmed H (2017) An experimental study of local scour around piers in the curved channels. *J Multidiscip Eng Sci Technol* 4(1):6448–6453
25. Maatooq JS, Mahmoud ES (2017) Local scour around single central oblong bridge piers located within 180° bend. *Int J Hydraul Eng* 6(1):16–23
26. Vaghefi M, Moghanloo M, Dehghan D, Keshavarz A (2017) Experimental study of the effect of base-level fall at the beginning of the bend on reduction of scour around a rectangular bridge pier located in the 180 degree sharp bend. *J Hydraul Struct* 3(2):32–46
27. Vaghefi M, Motlagh MJTN, Hashemi SS, Moradi S (2018) Experimental study of bed topography variations due to placement of a triad series of vertical piers at different positions in a 180° bend. *Arab J Geosci* 11(5):102–115. <https://doi.org/10.1007/s12517-018-3443-4>
28. Eghbalnik L, Vaghefi M, GolbaharHaghighi MR (2019) Laboratory study of the temporal evolution of channel bed topography in presence of two rows of inclined-vertical piers in a sharp 180-degree bend. *ISH J Hydraul Eng*. <https://doi.org/10.1080/09715010.2019.1674700>
29. Asadollahi M, Vaghefi M, Akbari M (2020) Effect of the position of perpendicular pier groups in a sharp bend on flow and scour patterns: numerical simulation. *J Braz Soc Mech Sci Eng* 42(8):1–15. <https://doi.org/10.1007/s40430-020-02503-2>
30. Mahmoud AH (2020) Effect of soil particle size in reducing the scour around bridge piers at the curved channels. *Life Sci J* 17(4):43–49. <https://doi.org/10.7537/marslsj170420.08>
31. Moghanloo M, Vaghefi M, Ghodsian M (2020) Experimental investigation on the effect of increasing the collar thickness on the flow pattern around the oblong pier in 180° sharp bend with balanced bed. *J Appl Fluid Mech* 13(1):245–260
32. Moghanloo M, Vaghefi M, Ghodsian M (2020) Experimental study on the effect of thickness and level of the collar on the scour pattern in 180° sharp bend with bridge pier. *Iran J Sci Technol Trans Civ Eng* 44(5):1–19. <https://doi.org/10.1007/s40996-020-00511-9>
33. Rasaei M, Nazari S, Eslamian S (2020) Experimental investigation of local scouring around the bridge piers located at a 90° convergent river bend. *Sadhana* 45(1):87–102. <https://doi.org/10.1007/s12046-020-1314-7>
34. Sedighi F, Vaghefi M, Ahmadi G (2020) The effect of inclined pair piers on bed topography: clear water, incipient motion and live bed. *Iran J Sci Technol Trans Civ Eng*. <https://doi.org/10.1007/s40996-020-00481-y>
35. Vaghefi M, Akbari M (2019) A procedure for setting up a 180-degree sharp bend flume including construction and examinations with hydraulic structures. *Sci Iran Trans A Civil Eng* 26(6):3165–3180
36. Chiew YM (1995) Mechanics of riprap failure at bridge piers. *J Hydraul Eng* 121(9):635–643. [https://doi.org/10.1061/\(asce\)0733-9429\(1995\)121:9\(635\)](https://doi.org/10.1061/(asce)0733-9429(1995)121:9(635))
37. Melville BW, Chiew YM (1999) Time scale for local scour depth at bridge piers. *Journal of Hydraulic Engineering ASCE* 125 (1): 59–65. [https://doi.org/10.1061/\(ASCE\)0733-9429](https://doi.org/10.1061/(ASCE)0733-9429)
38. Melville BW, Sutherland AJ (1988) Design method for local scour at bridge piers. *J Hydraul Eng* 114(10):1210–1226. [https://doi.org/10.1061/\(asce\)0733-9429\(1988\)114:10\(1210\)](https://doi.org/10.1061/(asce)0733-9429(1988)114:10(1210))

**Publisher's Note** Springer Nature remains neutral with regard to jurisdictional claims in published maps and institutional affiliations.